Journal of Geomatics Vol. 17, No. 1, April 2023

Spatiotemporal analysis of land surface temperature owing to NDVI: A case study of Vadodara District, Gujarat

Sharmistha Bhowmik* and Bindu Bhatt
The Maharaja Sayajirao University of Baroda, Vadodara
*Email: sharmib24031988@gmail.com

(Received: January 15, 2022; in final form Feb 20, 2023)

DOI- *https://doi.org/10.58825/jog.2023.17.1.83*

Abstract: The expeditious extension of LULC in the name of development is the root cause of global warming. Replacement of natural resources due to the expansion of manmade erections is accountable for the increase in LST of Earth's topography. The impression of change in LULC is reflected in LST. To seize the rising temperature, the lamentation of a new plan of action for urbanization is of utmost requisite. This paper examines the change in LULC and its spatiotemporal impact on LST in Vadodara, which is situated on the bank of river Vishmamitri river. Vadodara an arid region has three main seasons and these are summer, monsoon, and winter. The climate is characterized by hot summer and dryness in the non-rainy seasons. May is the hottest month while January is the coldest month. The annual rainfall of the district is 475.2 mm. Hence, to analyze we used multi-spectral and multi thermal Landsat TM and ETM+ satellite images to monitor the evaluation of LULC and its impact on LST from 2001(pre-monsoon) to 2021(pre- monsoon). The study explores to what extent observed LST can be examined by vegetation cover measured through NDVI from2001 to 2021. To achieve this an analysis of co-relation is performed between LULC and LST and by using spectral indices comprising NDVI with the help of software like ArcGIS 10.2 and Erdas Imagine 2014. It had been observed that a considerable increase in LST in Vadodara was 58.338°C (Max) and 21.9014°C (Min) in 2001(pre-monsoon) to 60.844 °C (Max) and 24.6784 °C (Min) in 2021(pre-monsoon) which is just about 2°C increase in Max and 3 degrees increase in Min for LST in past 20 years. It was also observed that there is an inverse relationship between LST and NDVI. The value of NDVI is observed that change from 0.380711(H) and -0.59322(L) in 2001 to 0.551(H) to -0.351193(L)in 2021. Moreover, SMI places a vital role to investigate and verify the relation between LST and NDVI. Henceforth, to verify SMI was also calculated and it was noticed that places with high LST value and low NDVI value contained less soil moisture and places with less LST value and high NDVI values contained more soil moisture. Thus, it can be concluded that, if urban planners and decision-makers implement suitable land-use strategies then Earth's topography can be protected from adverse effects of urban heat by planting adequate and appropriate trees in bare soil and beside the impervious areas, thus the expansion of UHI can also be controlled. Moreover, with the help of SMI values, it will also be beneficial for the agricultural sector.

Keywords: Land Use Landcover, Land Surface Temperature (LST), NDVI (Normalized Difference Vegetation Index), SMI (Soil Moisture Index).

1. Introduction:

The most important role it plays in the transmission of energy and water from the ground to the atmosphere is that of the land surface temperature (LST), which is an essential component in the physics of land surface processes (Jin et al., 1997; Yuvaraj, 2020). Therefore, the spatial and temporal distributions of LST reveal the changes in climatic factors and the characteristics of the landsurface (Yuvaraj, 2020). By, accurately studying and analyzing the combined factor of Land Surface Temperature with physical properties such as vegetation and soil moisture, we can access valuable metrics of surface state. Vegetation can effectively influence LST by selectively absorbing and reflecting solar radiation energy and regulating latent and sensible heat exchange (Yuvaraj, 2020). Land surface temperature, which is a significant parameter of the urban climate system,can be derived from satellite observations to monitor long-term environmental changes (Guillevic et al., 2012; Li et al., 2013; Voogt and Oke, 2003). Land Surface Temperature measurement is one of the desirable goals of satellite-based remote sensing in theTIR part of the electromagnetic spectrum (Shah et al., 2012). Using thermal infrared (TIR) remote sensing, environmental characteristics can be gathered, examined, and modeled (Feizizadeh and Blaschke, 2012). It makes it possible to figure out land surface temperature (LST), a crucial element in many environmental processes like global warming or urban heat (Feizizadeh and Blaschke, 2012). It's important to emphasize here that two key ways that TIR data help us understand land surface processes better: In addition to observed point data, surface temperature values can be associated with specific landscape and biophysical elements. They can also be related to energy fluxes of certain landscape phenomena or processes (Feizizadeh and Blaschke, 2012; Quattrochi and Luvall, 1999; Sobrino et al., 2006).

The technical term remote sensing was first coined by Evelyn Pruitt at the United States office research in 1958 (Estes and Jenson 1998; Yadav et al., 2016). The science and art of learning about an object, location, or p or phenomenon by analyzing data collected by a device that isn't in direct contact with the subject under study is referred to as remote sensing (Lillesand and Kiefer, 1979; Tomlinson et al., 2011). Usage is growing within the fields of meteorology and climatology and works in unison with the use of Geographical Information Systems (GIS) for spatial analysis (Chapman and Thornes, 2003; Dyras et al., 2005; Tomlinson et al., 2011). However, the identification of the

patterns and analyses of spatial and temporal changes would help immensely in the planning for proper infrastructural facilities (Igbokwe et al., 2013).This could be done effectively and efficiently with the help ofspatial and temporal technologies such as GIS and Remote sensing, along with collateral data such as surveys of existingmaps, etc. (Barnes et al., 2001). Remote sensing also provides a sound database for generating baseline information on natural resources and a prerequisite for planning and implementing, and monitoring any developmental program (Yadav et al., 2016). Further, the application of the Geographical Information System (GIS) inanalyzing the trends and estimating the changes that have occurred in different themes helps in the management decision-making process (Yadav et al., 2016).

In general, NDVI values range from -1 to 1 (GIS Geography, 2018). Vegetation is healthier when the NDVI values are high. Low NDVI means there is little to no vegetation present (GIS Geography, 2018). The proportion of the field capacity and the remaining soil moisture to the difference between the current soil moisture and the permanent wilting point is known as the soil moisture index (SMI) (Saha et al., 2018). Soil moisture is the total amount of water present in the upper 10 cm of soil and it represents the water on the land surface that resides in the pores of the soil which is not in rivers, lakes, or groundwater and which and which depends on the weather conditions, soil type, and associated vegetation, among others (Gonzalez, 2021). Surface temperature is also regulated by soil moisture levels because evaporation is a more efficient cooling mechanism than sensible heating (Bateni and Entekhabi, 2012). To explore the changes in LST under different vegetation coverconditions the relation between summer LST with NDVI and SMI of pre-monsoon 2001 and 2021 was selected to investigate the impacts.

2. Study Area:

Vadodara district is part of the great Gujarat plain. Vadodaradistrict with a 7548 sq. km area is located in the central part of the mainland of Gujarat between 21°49’19” and 22°48’37” north latitude and 72°51’05” and 74°16’55” east longitude. Vadodara district is bounded in the north and northeast by Anand,Panchmahals, and Dahod districts in the east and the southeast by Madhya Pradesh and Maharashtra, in the southeast by Narmadadistrict and in the south and the west by Bharuch district. The western and southern portion of the Vadodara district is comprised of Mahi and Narmada Doab which is an alluvial plain region with gently undulating terrain. The central portion of the district is comprised of an undulating plain with a low-level plateau and a few relict hills. The existence of a low-level stabilized dune with rolling topography is noticed in the central area between the Unch river and the Orsang river. The eastern and northeastern portion of the district is hilly terrain with few ridges, flat-topped plateaux, and isolated relict hills.

3. Materials and Methods:

3.1 Data Acquired:

Landsat 7 ETM+ and Landsat 8 OLI_TIRS were used to calculate LST, NDVI, and SMI for the study purpose.The digital data sets used in the present study were created by the USGS and were acquired in GeoTIFF (Nasar and Minallah, 2020). The optical bands of satellite Landsat 7 and 8 were utilized in developing NDVI and SMI. Georeferencing was done using the UTM projection method for Landsat images (WGS 1984, Zone 43N). Moreover, the nearest-neighbor algorithm was used for resampling with the size of a pixel of30m*30m. ERDAS Imagine and ArcGIS 10.6 were used to analyze the satellite data and acquire the concluding product during the whole study.

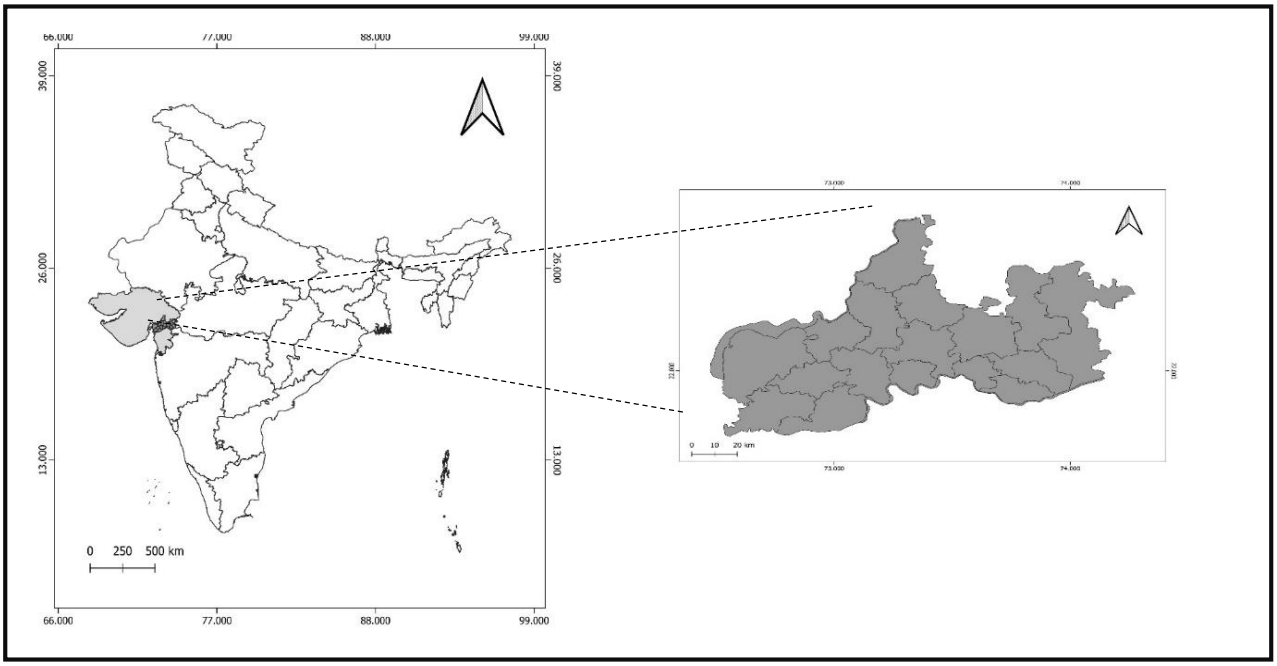

Figure 1. Location Map of The Study Area

3.2 Calculating LST, NDVI, and SMI:

3.2.1 Converting Digital Numbers (DN) to Top of Atmospheric Spectral Radiance (TOA):

The algorithm's initial stage is the input of Band 10. The program uses algorithms from the USGS website to retrieve the top of atmospheric (TOA) spectral radiation after band 10 is entered in the background (Lλ):

$$L\lambda = M_L * Q_{cal} + A_L - O_i, \quad (1)$$

Where Q_{cal} is the Band 10 image, A_L is the band-specific additive rescaling factor, M_L represents the band-specific multiplicative rescaling factor, and $O_i$is the Band 10 correction (Avdan and Jovanovska, 2016; Barsi et al., 2014).

The TIRS band data should be converted from spectral radiance to brightness temperature (BT) using the thermal constants provided in the metadata file after the digital numbers (DNs) are translated to to reflection. The tool's algorithm converts reflectance to BT using the following equation (Avdan and Jovanovska, 2016).

$$BT = \frac{K_2}{1_n\,[(K_1/L_\lambda)+1]} - 273.15 \quad (2)$$

Seen from metadata, where $K_1$and K_2 stand for the band-specific thermal conversion constants. The radiant temperature is corrected by adding absolute zero (about 273.15°C) to obtain the figures in Celsius (Xu and Chen, 2004).

3.2.2 Calculating NDVI:

Since NDVI can be used to infer overall vegetation condition, it is crucial to estimate it since the amount of vegetation present is a crucial element.

$$NDVI = \left(\frac{NIR-RED}{NIR+RED}\right) \quad (3)$$

In contrast to other wavelengths, healthy vegetation (chlorophyll) reflects greener and near-infrared (NIR) light. It does, however, absorb more red and blue light (GIS Geography, 2022).

3.2.3 Calculating the Proportion of Vegetation:

The proportion of vegetation (Vegetation Fraction) is defined as the percentage of vegetation occupying the ground area invertical projection (Twumasi et al., 2021). The proportion of vegetation P_V is closely related to NDVI values for vegetation and soil. In this study, PV was estimated following the NDVI traditional method (Rouse et al., 1974; Twumasi et al., 2021). The NDVI algorithm makes use of the fact that dense or less green vegetation reflects more visible light and less near-IR, while green vegetation reflects less visible light and more NIR Dutta 2016).

$$P_v = \left[\frac{NDVI-NDVI_s}{NDVI_v-NDVI_s}\right]^2 \quad (4)$$

where $NDVI_v$ and $NDVI_s$ are Maximum and Minimum $NDVI$ respectively, representative of NDVI of Vegetation and NDVI of soil respectively (Bendib et al., 2017; Carlson and Ripley, 1997).

3.2.4 Calculating Land Surface Emissivity:

Since LSE is a proportionality factor that scales blackbody radiance (Plank's Law) to predict emitted radiance and represents the effectiveness of transporting thermal energy across the surface into the atmosphere, it is the key component in the computation of LST (MuñozJiménez-Juan C. et al., 2006).

The emissivity calculation formula looks like this:

$$\varepsilon\lambda = \varepsilon v\lambda \mathrm{P}v + \varepsilon s\lambda\,(1 - \mathrm{P}v) + C\lambda \quad (5)$$

Where C denotes the surface roughness assumed as a constant value and $\boldsymbol{v}$ and $\boldsymbol{s}$ are the vegetation and soil emissivities, respectively (Avdan and Jovanovska, 2016).

3.2.5 Calculating LST (Land Surface Temperature):

The "surface" of the Earth would feel warm when touched in that area can be defined as LST. The "surface" is anything a satellite observes when it peers through the atmosphere to the earth. It might be ice and snow, grass on a lawn, a building's roof, or the leaves in a forest canopy. LST and the air temperature listed in the daily weather report are different" .

$$LST = \frac{T_B}{1+\left(\lambda\sigma T_B/(hc)\right)ln\varepsilon} \quad (6)$$

where: $h\,is$ Plank's constant (6.626 1034 Js), $\sigma\,is$ the Boltzmann constant (1.38 1023 J/K), $c\ is$ the velocity of light in a vacuum (2.998 108 m/sec), $\lambda\,is$ the effective wavelength (10.9 mm for band 10 in Landsat 8 data), and ε is the emissivity are all constants. (Guha et al., 2018; Weng et al., 2004)

3.3 Calculating SMI:

Soil moisture is always an important factor in agriculture, certainly in semi-arid and arid circumstances (Arnold, 1999; Enkhjargal Natsagdorj, 2021) Determination of SMI (Soil Moisture Index) is an effective factor in biological processes and soil profile evolution. In addition, soil moisture affects vegetation distribution (Mohamed et al., 2020). The SMI has been retrieved directly according to (Moawad, 2012) using LST as follows for Landsat 8:

$$SMI = \left(\frac{LST_{max}-LST}{LST_{\max}-LST_{min}}\right) \quad (7)$$

where LST_{max}, LST_{min}, LST and are the maximum, minimum, and value of the recovered LST in turn, and SMI stands for Soil Moisture Index.

The SMI has been retrieved directly according to (Dupigny-Giroux et al., 1999; Enkhjargal Natsagdorj, 2021) for Landsat 7 as follows:

$$SMI = \frac{NIR}{VisBlue} \quad (8)$$

where band 1 is $VisBlue$ and band 4 is NIR.

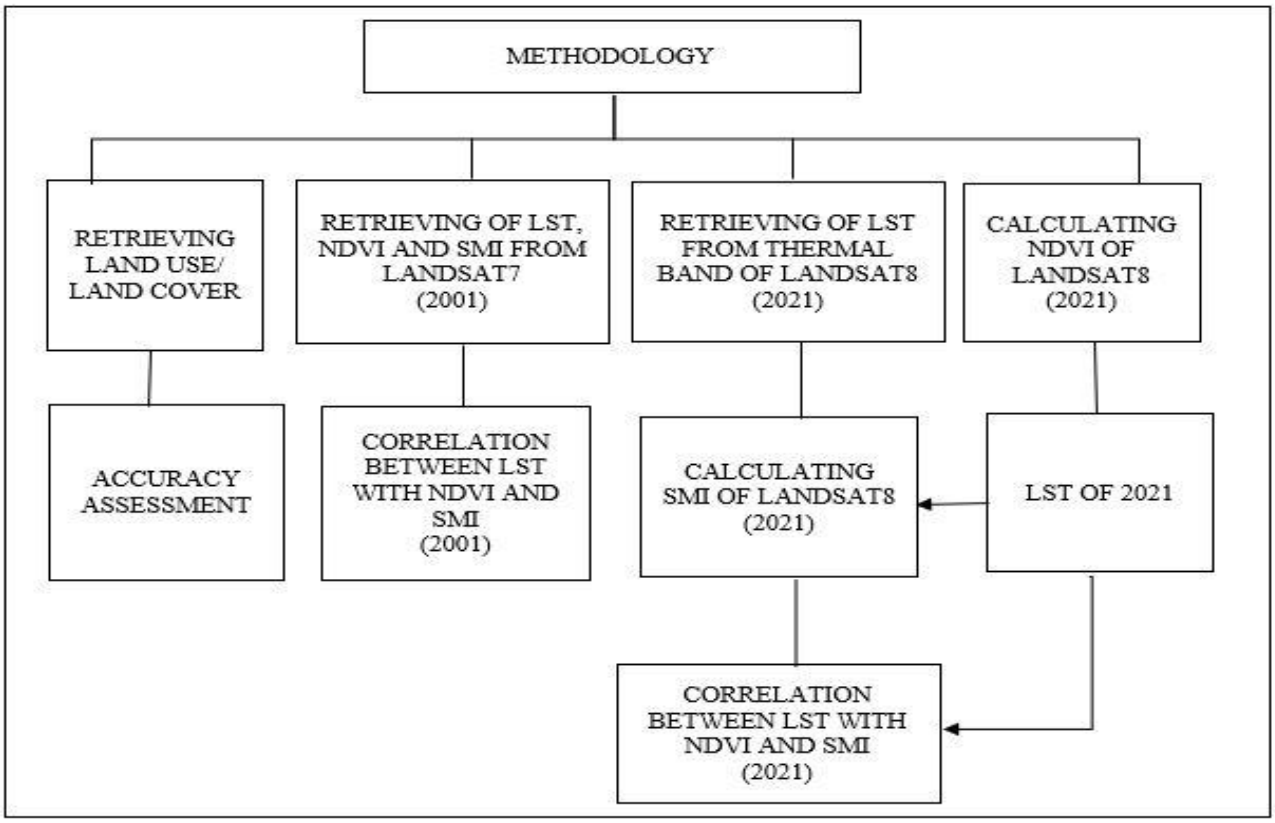

Figure 2. Flowchart of Methodology

4. Results:

The increasing population has changed the land cover pattern through overexploitation of land resources for their livelihood because the population residing near forests depends on valuable timber for forest and agriculture (Bhattacharjee and Nayak 2003; Das and Joshi 2013). The pressure of increasing population and unplanned land use practices has a great impact on natural land cover. The change in land use and land cover also disturbs the other natural components of soil fertility, soil erosion, ecology, biodiversity, air quality, and water regime of the distributed area (Singh and Singh, 2016).

Kappa for 2001 was 0.91, for 2006 it was 0.92, 0.90 for 2011, 0.92 for 2016 and 0.94 for 2021.

4.1 LULC Analysis:

LULC of 2001, 2006, 2011, 2016, and 2021 is described below in Fig. 3, and meta data are available in Table 1. Change detection of LULC is also performed and metadata are available in Table 2.

Table 1. Table showing LULC types and their area in sq. km.

LULC Type	2001 area sq. km.	2006 area sq. km.	2011 area sq. km.	2016 area sq. km.	2021area sq. km.
Bare Soil	5223.92	4682.18	3724.76	3273.58	2710.19
Fallow land	3211.36	3392.53	3428.11	3533.49	3366.08
Settlement	1087.62	1357.71	1780.86	1998.91	2365.61
Vegetation	807.36	892.76	1394.94	1511.85	1869.46
Water body	466.92	472.00	468.51	479.35	485.84

Table 2. Table showing change in area of LULC type

LULC Type	2001 to 2006 area changed	2006 to 2011 area changed	2011 to 2016 area changed	2016 to 2021 area changed
Bare Soil	-541.74	-957.42	-451.18	-563.39
Fallow land	181.17	35.58	105.38	-167.41
Settlement	270.09	423.15	218.05	366.70
Vegetation	85.40	502.18	116.91	357.61
Water body	5.08	-3.49	10.84	6.49

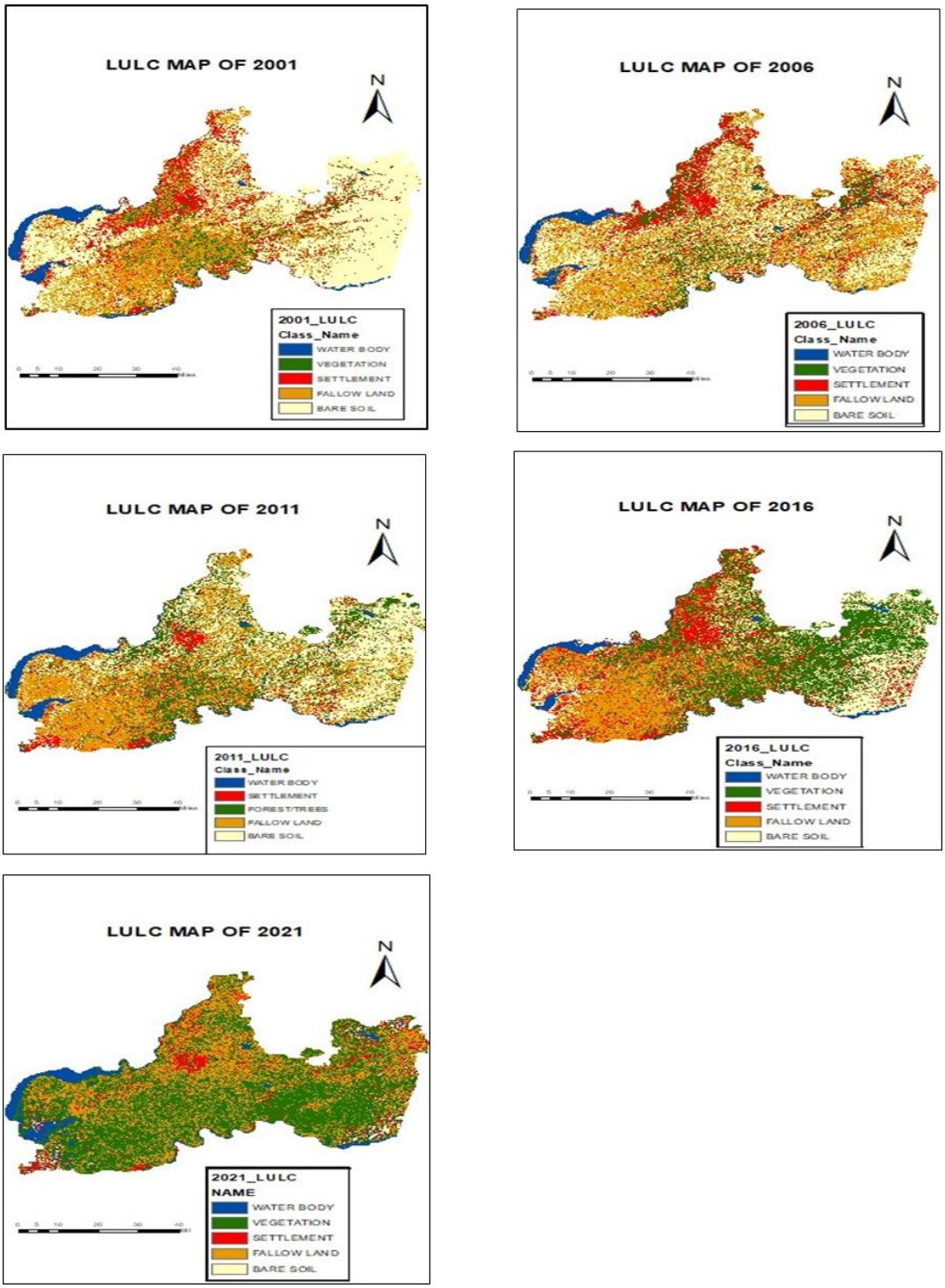

Figure 3. LULC Map of 2001, 2006, 2011, 2016, and 2021.

From the LULC maps, it can be analyzed that blue color represents water bodies, red represents settlements or built-up, vegetation is represented by green color, brown color represents fallow land and off-white color represents bare soil. From 2001 to 2006 bare land decreased, as it was replaced by settlements, especially in the urban area, and it was also replaced by fallow lands in the eastern zone of the district. Forest, big trees were replaced by settlements in urban areas. However, the existence of small shrubs and plants were noticed around settlements, roads, and other built-up areas. From 2016 to 2011 too bare land decreased and it was replaced by fallow land and settlements. Here also, small trees or plants was observed to have replaced bare soil, which were planted near new settlements and along the roadside. The same trend was observed from 2011 to 2016 and from 2016 to 2021, but, fallow lands which decreased, was replaced by vegetation. In the year 2021 vegetation is observed to be higher than in all other years, firstly because of the increasing trend of plantation and moreover due to the high amount of rainfall in 2020 post-monsoon. Rainwater increases soil moisture which may have helped in the growth of bushes and shrubs. Water bodies more or less remained constant.

4.2 Analysis of LST, NDVI, and SMI

4.2.1 LST:

The distribution of LST in Fig. 4 illustrates that black color represents high temperature, grey represents medium temperature and white represents low temperature. The high temperature was observed in barren lands and in settlement areas. Whereas, forested areas and areas covered with vegetation and water bodies registered low temperatures

4.2.2 NDVI:

The distribution of NDVI is illustrated in Fig.5. Black represents high NDVI with a value near +1, grey represents medium temperature whereas white represents low NDVI with a value near -1. High NDVI was observed in agricultural lands, as well as forested areas. Whereas, barren areas and areas with fallow land, built-up areas, and water bodies prevail in low NDVI.

4.2.3 SMI:

The distribution of SMI in Fig.6 illustrates a value near 1 with black representing high SMI, greyresenting medium SMI, and white representing low SMI with avalue near 0. High SMI was observed in agricultural lands, aswell as forested areas. Low SMI prevails in the settlement and fallow land areas.

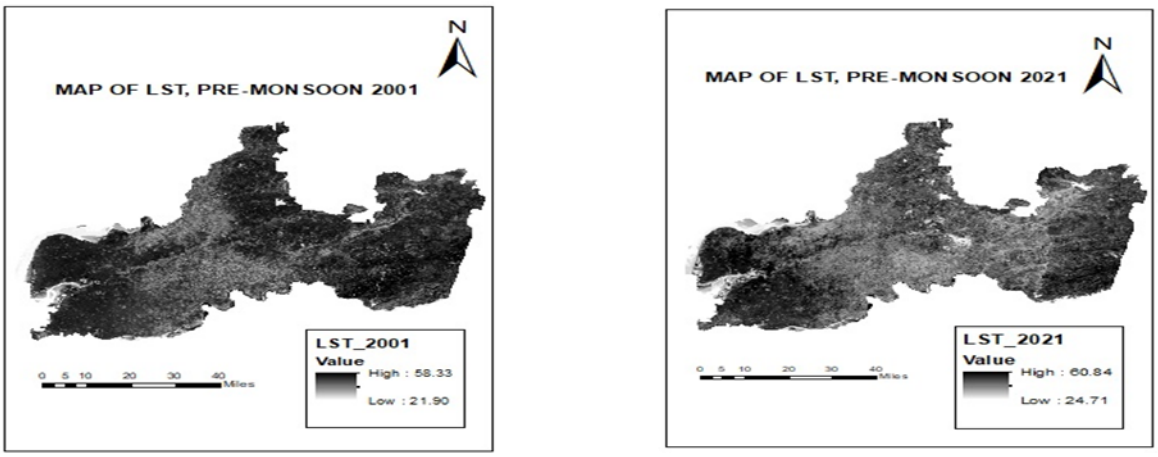

Figure 4. LST Map of 2001 and 2021

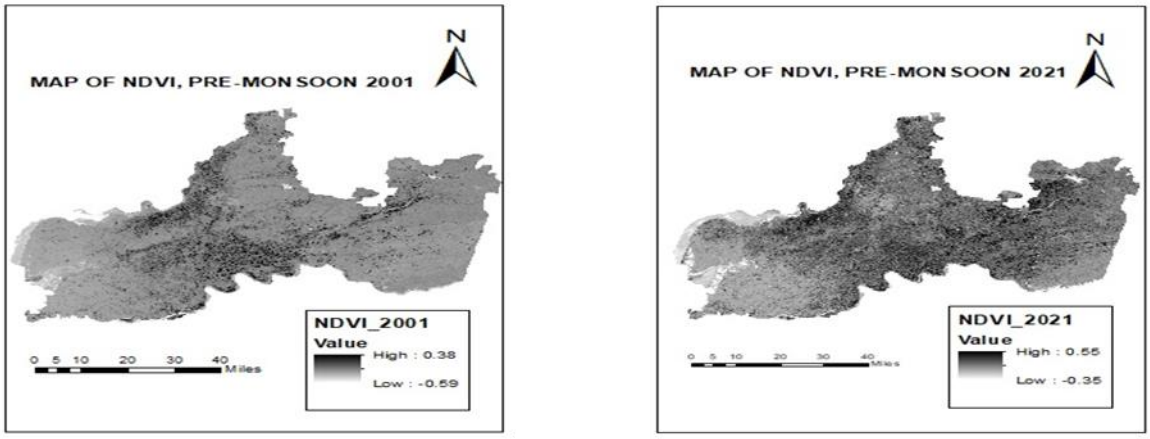

Figure 5. NDVI Map of 2001 and 2021

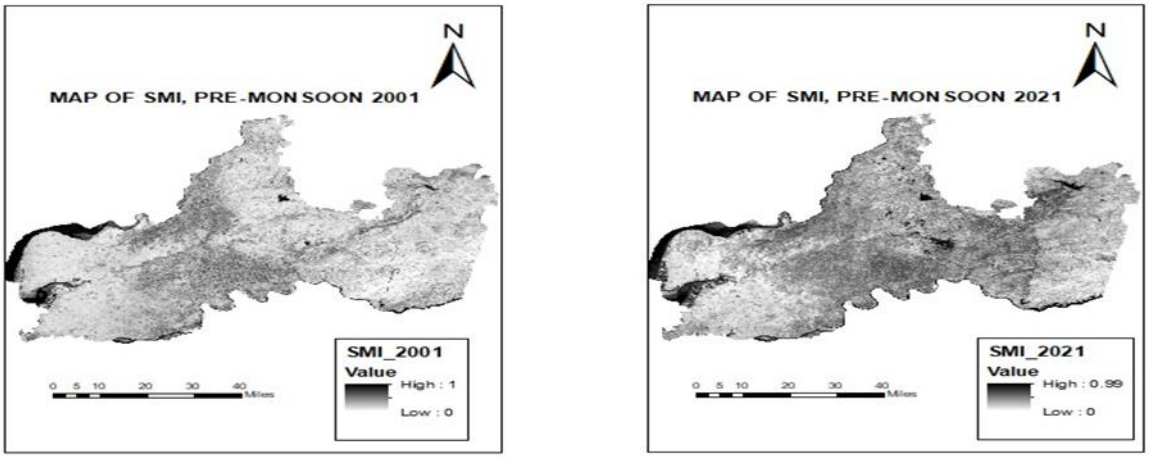

Figure 6. SMI Map of 2001 and 2021

4.3 Correlation between LST with NDVI and SMI:

In 2001 high value of LST was observed to be 58.33 ℃ and the low value was 21.90 ℃. In 2021 the high value of LST changed to 60.84 ℃ and the low value changed to 24.71 ℃. In the case of NDVI in 2001 the high value was recorded as 0.38 and the low value as -0.59 and in 2021 the high value changed to 0.55 and the low value changed to -0.35. The high value of SMI was 1 and the low value was 0 in 2001. The high value of SMI was 0.99 and the low value was 0 in 2021. In 2001 mean LST was 36.33^{o} C and mean NDVI was -0.23 and the mean value of SMI was 0.51 whereas in 2021 mean LST increased to 39.76. On the other hand, the mean value of NDVI increased from -0.23 to 0.19. Moreover, the mean value of SMI increased to 0.68. This study has analyzed the Land Surface Temperature of theVadodara district of Gujarat in the years 2001 (pre-monsoon)and 2021 (pre-monsoon). The results indicated that the eastern zone with barren hilly rugged hills and fallow lands in the southwestern zone is distributed by high Land Surface Temperature (LST) and the central zone and the northeastern zone are distributed by low LST owing to the existence of high vegetation as agriculture is practiced in settlement areas as well as areas adjacent to rivers and water bodies. It is also noticed that vegetation and water body is inversely related to LST and built-up and bare soil has a positive relationship with LST. Furthermore, it is crucial to note that LST is impacted by urban growth and that vegetation is seen as a key role in reducing the intensity of urban heat islands. The Correlation is depicted in Fig. 7

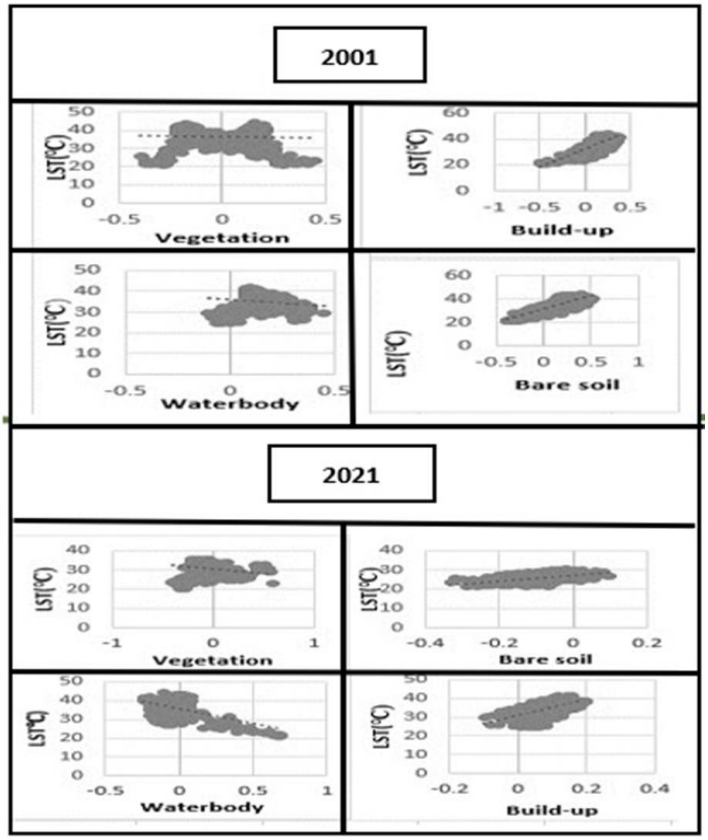

Figure 7. Correlation between LST with vegetation, built-up, water-body and bare soil (2001, 2021)

5. Conclusion:

The LST distribution of the Vadodara district was characterized by a warmer western and eastern zone and a cooler zone adjacent to water bodies and areas occupied by vegetation. Mean LST over the period of 20 years increased by just 3ºC. For the study purpose, LST NDVI and SMI had been utilized. Normalized difference vegetation index (NDVI) is a vegetation identifier in the area that is purposefully utilized in the study to find the relationship with LST (Deng et al., 2018). It was observed that the value of NDVI increased from 2001 to 2021 in the Vadodara district. It was also analyzed that Soil Moisture Index was high where there existed high vegetation. A value close to zero indicates water deficiency and a value near 1 indicates a forested area that has more moisture compared to the rest of the land cover. Wet soil increases evaporate fraction, lowering the surface temperature and thereby decreasing the longwave radiation emitted by the surface. (Ballinas and Barradas, 2016) explains that 24 large trees can reduce air temperature by two degrees (Rushayati et al., 2018). The initiatives taken by the Gujarat government have helped to increase the vegetation cover over the period. Social forestry programs/schemes for like planting in strip lands like, along the roadside, railway side, and canal banks, planting in degraded lands, government wastelands, check to gaze in villages, fruit tree plantations through farmer's participation, Rehabilitation of Degraded Farm Land (RDFL) helped in increasing the ratio of vegetation cover in Vadodara district (Principal Chief Conservator of Forest and Head of the Forest Force (HoFF), 2020). It was also observed that Drip Irrigation was created in Gaucher Land and Barren Hillocks Land. Narmada Irrigation Project has helped in the adoption of horticulture crops, fruits, and vegetables by farmers. About 10 hectares of land have been collectively dedicated to growing grapes in Savli village in the Vadodara district, and the early results are comparable to those of any other region of the nation (Thakkar, 2013). Trees and vegetation lower surface and air temperature by lowering surface and air temperatures by providing shade and evapotranspiration. The Soil Moisture index is an important parameter for the production of vegetation. Hence, if proper care is taken for mother earth by increasing plantations Global Warming can be controlled. May the study prove useful for urban planners to mitigate the accelerating LST by reducing some of the impacts of urban development.

Acknowledgment:
The authors are grateful to SHODH- ScHeme of Developing High quality research, Education Department, Gujarat State for the fellowship provided.

References:

Arnold J.E. (1999). *SOIL MOISTURE*. https://weather.msfc.nasa.gov/landprocess/

Avdan U. and G. Jovanovska (2016). Algorithm for automated mapping of land surface temperature using LANDSAT 8 satellite data. *Journal of Sensors, 2016*. https://doi.org/10.1155/2016/1480307

Ballinas, M. and V.L. Barradas (2016). The Urban Tree as a Tool to Mitigate the Urban Heat Island in Mexico City: A Simple Phenomenological Model. *Journal of Environmental Quality*, *45*(1). https://doi.org/10.2134/jeq2015.01.0056

Barnes K., J. Morgan, M. Roberge and S. Lowe (2001). Sprawl Development: Its Patterns, Consequences, and Measurement. *Annals of Physics*, *54*.

Barsi J. A., J.R. Schott, S.J. Hook, N.G. Raqueno, B.L. Markham and R.G. Radocinski (2014). Landsat-8 thermal infrared sensor (TIRS) vicarious radiometric calibration. *Remote Sensing*, *6*(11). https://doi.org/10.3390/rs61111607

Bateni S. M. and D. Entekhabi (2012). Relative efficiency of land surface energy balance components. *Water Resources Research*, *48*(4). https://doi.org/10.1029/2011WR011357

Bendib A., H. Dridi and M.I. Kalla (2017). Contribution of Landsat 8 data for the estimation of land surface temperature in Batna city, Eastern Algeria. *Geocarto International*, *32*(5). https://doi.org/10.1080/10106049.2016.1156167

Bhattacharjee P.R and P. Nayak (2003). Socio-economic rationale of a regional development council for the Barak Valley of Assam. *Journal of NEICSSR, 27(1),* 13–26. https://www.researchgate.net/publication/267765309_A_remote_sensing_study_for_land_cover_change_in_south_Assam_India

Carlson T. N. and D.A. Ripley (1997). On the relation between NDVI, fractional vegetation cover, and leaf area index. *Remote Sensing of Environment*, *62*(3). https://doi.org/10.1016/S0034-4257(97)00104-1

Chapman L. and J.E. Thornes (2003). The use of geographical information systems in climatology and meteorology. *Progress in Physical Geography*, *27*(3). https://doi.org/10.1191/030913303767888464

Das P., & S. Joshi. (2013). A remote sensing study for land cover change in south Assam, India. *Earth Science India*, *6 (lll)*, 136–146. https://www.researchgate.net/publication/267765309_A_remote_sensing_study_for_land_cover_change_in_south_Assam_India

Deng, Y., S. Wang, X. Bai, Y. Tian, L. Wu, J. Xiao, F. Chen and Q. Qian. (2018). Relationship among land surface temperature and LUCC, NDVI in typical karst area. *Scientific Reports*, *8*(1). https://doi.org/10.1038/s41598-017-19088-x

Dupigny-Giroux, L. and J. E. Lewis. (1999). A Moisture Index for Surface Characterization over Semi-Arid Area. *Photogrametric Engineering Remote Sensing*, *65*(8), 937–945. https://www.asprs.org/wpcontent/uploads/pers/1999journal/aug/1999_aug_937-945.pdf

Dutta R. (2016). *Review of Normalized Difference Vegetation Index (NDVI) as an Indicator of Drought*.

Dyras I., H. Dobesch, E. Grueter, A. Perdigao, O.E. Tveito, J.E. Thornes, F. van der Wel and I. Bottai (2005).

The use of Geographic Information Systems in climatology and meteorology: COST 719. *Meteorological Applications*, *12*(1). https://doi.org/10.1017/S1350482705001544

Enkhjargal Natsagdorj. (2021). *Soil moisture analysis using remotely sensed data in the agricultural region of Mongolia* [GHENT UNIVERSITY]. https://www.researchgate.net/publication/351225146_Soil_moisture_analysis_using_remotely_sensed_data_in_the_agricultural_region_of_Mongolia

Estes J. and Jensen. (1998). Development of remote sensing digital image processing systems and raster GIS. *The History of Geographic Information Systems. Longman, New York*, 163–180.

Feizizadeh B. and T. Blaschke (2012). Thermal remote sensing for land surface temperature monitoring: Maraqeh County, Iran. *International Geoscience and Remote Sensing Symposium (IGARSS)*. ttps://doi.org/10.1109/IGARSS.2012.6350808

GIS Geography. (2018). What is NDVI (Normalized Difference Vegetation Index)? *Web Page GIS Geography*.

GIS Geography. (2022). *What is NDVI (Normalized Difference Vegetation Index)?* https://gisgeography.com/ndvi-normalized-difference-vegetation-index/

Gonzalez R.R. (2021). *Landsat 8 satellite data-based estimation of soil moisture in McMurdo Dry Valleys, Antarctica*. https://run.unl.pt/bitstream/10362/113892/1/TGEO0270.pdf

Guha, S., H. Govil, A. Dey and N. Gill (2018). Analytical study of land surface temperature with NDVI and NDBI using Landsat 8 OLI and TIRS data in Florence and Naples city, Italy. *European Journal of Remote Sensing*, *51*(1). https://doi.org/10.1080/22797254.2018.1474494

Guillevic P. C., J.L. Privette, B. Coudert, M.A. Palecki, J. Demarty, C. Ottlé and J.A. Augustine (2012). Land surface temperature product validation using NOAA's surface climate observation networks-scaling methodology for the visible infrared imager radiometer suite (VIIRS). *Remote Sensing of Environment*, *124*. https://doi.org/10.1016/j.rse.2012.05.004

https://www.business-standard.com/article/economy-policy/narmada-water-changing-crop-pattern-in-the-region-105021601093_1.html

Igbokwe J.I, I.C. Ezeomedo and J. Ejikeme (2013). Identification of Urban Sprawl Using Remote Sensing and GIS Technique: A Case Study of Onitsha and Its Environs in South East Nigeria. *Environmental Science, Mathematics*, *2*, 41–49.

Jin, M, R. E. Dickinson and A.M. Vogelmann (1997). A comparison of CCM2-BATS skin temperature and surface-air temperature with satellite and surface observations. In *Journal of Climate* (Vol. 10, Issue 7).

Li, Z. L., B.H. Tang, H. Wu, H. Ren, G. Yan, Z. Wan, I.F. Trigo and J.A. Sobrino (2013). Satellite-derived land surface temperature: Current status and perspectives. In *Remote Sensing of Environment* (Vol. 131). https://doi.org/10.1016/j.rse.2012.12.008

Lillesand, T.M. and R.W. Kiefer (1979). Remote sensing and image interpretation. *Remote Sensing and Image Interpretation.* https://doi.org/10.2307/634969

Moawad B.M. (2012). *Geoscience general tool package*. https://www.sciencedirect.com/science/article/pii/S1110982318304551#b9045

Mohamed E. S., A. Ali, M. El-Shirbeny, K. Abutaleb and S. M. Shaddad (2020). Mapping soil moisture and their correlation with crop pattern using remotely sensed data in arid region. *Egyptian Journal of Remote Sensing and Space Science*, *23*(3). https://doi.org/10.1016/j.ejrs.2019.04.003

MuñozJiménez- Juan C., S. José A., G. Alan, S. Donald and W.T. Gustafson. (2006). Improved land surface emissivities over agricultural areas using ASTER NDVI. *Remote Sensing of Environment*, 474–487.

Nasar U and M. Minallah (2020). Exploring the Relationship between Land Surface Temperature and Land Use Change in Lahore Using Landsat Data. *Pakistan Journal of Scientific and Industrial Research Series A: Physical Sciences*, *63*(3). https://doi.org/10.52763/pjsir.phys.sci.63.3.2020.188.200

Principal Chief Conservator of Forest & Head of the Forest Force (HoFF), G. of G. (2020). *Schemes*. https://forests.gujarat.gov.in/schemes-details.htm

Quattrochi, D. A. and J. C. Luvall (1999). Thermal infrared remote sensing for analysis of landscape ecological processes: Methods and applications. *Landscape Ecology*, *14*(6). https://doi.org/10.1023/A:1008168910634

Rouse J.W., R.W. Haas, J.A. Schell, D.W. Deering and J.C. Harlan (1974). *Monitoring the Vernal Advancements (Greenwave Effect) and Retrogradation of Natural Vegetation.* https://ntrs.nasa.gov/citations/19740022555

Rushayati, S. B., A.D. Shamila and L.B. Prasetyo (2018). The Role of Vegetation in Controlling Air Temperature Resulting from Urban Heat Island. *Forum Geografi*, *32*(1). https://doi.org/10.23917/forgeo.v32i1.5289

Saha A., M. Patil, V.C. Goyal and D.S. Rathore (2018). *Assessment and Impact of Soil Moisture Index in Agricultural Drought Estimation Using Remote Sensing and GIS Techniques*. https://doi.org/10.3390/ecws-3-05802

Shah D. B., M.R. Pandya, H.J. Trivedi and A.R. Jani (2012). Estimation of minimum and maximum air temperature using MODIS data over Gujarat. In *Journal of Agrometeorology* (Vol. 14, Issue 2).

Singh R.P. and N. Singh. (2016). Normalised Difference Vegetation Index (NDVI) Based Classification to Access the Change in Land Use/Landcover (LULC) in Lower Assam, India. *School of Environmental Science*. https://www.researchgate.net/publication/315943042_Normalized_Difference_Vegetation_Index_NDVI_Based_Classification_to_Assess_the_Change_in_Land_UseLand_Cover_LULC_in_Lower_Assam_India

Sobrino J. A., J.C. Jiménez-Muñoz, P.J. Zarco-Tejada, G. Sepulcre-Cantó and E. de Miguel(2006). Land surface temperature derived from airborne hyperspectral scanner thermal infrared data. *Remote Sensing of Environment*, *102*(1–2). https://doi.org/10.1016/j.rse.2006.02.001

Thakkar M. (2013, March 1). Narmada water changing crop pattern in the region. *Business Standard*.

Tomlinson C. J., L. Chapman, J.E. Thornes and C. Baker (2011). Remote sensing land surface temperature for meteorology and climatology: A review. In *Meteorological Applications* (Vol. 18, Issue 3). https://doi.org/10.1002/met.287

Twumasi Y. A., E.C. Merem, J.B. Namwamba, O.S. Mwakimi, T. Ayala-Silva, D.B. Frimpong, Z.H. Ning, A.B. Asare-Ansah, J.B. Annan, J. Oppong, P.M. Loh, F. Owusu, V. Jeruto, B.M. Petja, R. Okwemba, J. McClendon-Peralta, C.O. Akinrinwoye and H.J. Mosby (2021). Estimation of Land Surface Temperature from Landsat-8 OLI Thermal Infrared Satellite Data. A Comparative Analysis of Two Cities in Ghana. *Advances in Remote Sensing*, *10*(04). https://doi.org/10.4236/ars.2021.104009

Voogt, J. A. and T.R. Oke (2003). Thermal remote sensing of urban climates. *Remote Sensing of Environment*, *86*(3). https://doi.org/10.1016/S0034-4257(03)00079-8

Weng, Q., D. Lu and J. Schubring (2004). Estimation of land surface temperature-vegetation abundance relationship for urban heat island studies. *Remote Sensing of Environment*, *89*(4). https://doi.org/10.1016/j.rse.2003.11.005

Xu H. Q. and B.Q. Chen (2004). Remote sensing of the urban heat island and its changes in Xiamen City of SE China. *Journal of Environmental Sciences*, *16*(2).

Yadav, K. K., N. Gupta and V. Kumar (2016). Remote Sensing and Geographical Information System (GIS) and Its Applicationn in Various Fields. *American String Teacher*, *66*(1).

Yuvaraj R. M. (2020). Extents of Predictors for Land Surface Temperature Using Multiple Regression Model. *Scientific World Journal*, *2020*. https://doi.org/10.1155/2020/3958589